Molecular orientation and optical anisotropy in drawn films of cellulose diacetate-*graft*-PLLA: comparative investigation with poly(vinyl acetate-*co*-vinyl alcohol)-*graft*-PLLA

Takeshi Unohara, Yoshikuni Teramoto, Yoshiyuki Nishio*

Division of Forest and Biomaterials Science, Graduate School of Agriculture, Kyoto University, Sakyo-ku, Kyoto 606-8502, Japan

Phone: +81-75-753-6250

Fax: +81-75-753-6300

E-mail: ynishio@kais.kyoto-u.ac.jp

Abstract Cellulose diacetate-*graft*-poly(L-lactide) (CDA-*g*-PLLA) and poly(vinyl acetate-*co*-vinyl alcohol)-*graft*-PLLA (P(VAc-*co*-VOH)-*g*-PLLA) were synthesized over a range of compositions, by ring-opening copolymerization of L-lactide at the original hydroxyl positions of the respective trunk polymers, CDA (acetyl DS = 2.15) and P(VAc-*co*-VOH)-*g*-PLLA (VAc = 64.2 mol%). All the products of both graft copolymer series were non-crystallizable and their solution-cast films showed no domain segregation of the two components that constituted the trunk and side-chains. A comparative study on the molecular orientation and optical anisotropy induced by uniaxial stretching of film samples was undertaken for the two copolymer series with various side-chain lengths. Overall behaviour of the orientation was estimated from the statistical second ($<\cos^2 \omega>$) and fourth ($<\cos^4 \omega>$) moments obtained by a fluorescence polarization method using a rod-like probe of ~2.5 nm. Upon stretching, any film of both series imparted a positive orientation function, i.e., $f = (3<\cos^2 \omega> - 1)/2 > 0$, which increased with the extent of deformation. The degree of molecular orientation was higher in the CDA-graft series with a semi-rigid trunk, and, in both series, it declined monotonically with increasing content of the PLLA side-chain. With regard to the optical anisotropy, CDA-*g*-PLLA films always exhibited a positive birefringence ($\Delta n > 0$) upon stretching, while drawn films of P(VAc-*co*-VOH)-*g*-PLLA displayed a negative one. This contrast in polarity reflects a difference in the intrinsic birefringence between the two trunk polymers. Of interest was the finding of a discontinuous change in Δn value with copolymer composition (PLLA content) for the respective graft series, when compared at a given stage of elongation of the films. Discussion took into consideration the locally different orientation manners of the attached PLLA chain segments.

Keywords *cellulose acetate • poly(vinyl acetate-co-vinyl alcohol) • poly(L-lactide) • graft copolymer • molecular orientation • optical anisotropy*

Introduction

Graft copolymerization of cellulosics is one way to incorporate different polymer ingredients at a hyperfine structural level. It is now appreciated as a useful method not only of improving some of the original properties of polysaccharides, but also of allowing the product copolymers to exhibit a novel functionality. In recent years, the authors have carried out systematic works for synthesizing biodegradable cellulose ester-*graft*-aliphatic polyesters, through adoption of a homogeneous reaction system and complete removal of a possible oligomeric by-product of the grafting component (Teramoto and Nishio 2003; Teramoto et al. 2004; Nishio 2006). Various approaches in this regard have dealt with chemical composition and thermal transition behaviour (Teramoto and Nishio 2003; Teramoto et al. 2004), mechanical properties (Teramoto and Nishio 2003), higher-order structure development (Teramoto and Nishio 2004b; Kusumi et al. 2008), and enzymatic hydrolysis behaviour (Teramoto and Nishio 2004a; Kusumi et al. 2009).

The particular focus of this paper is on the orientation behaviour and optical anisotropy of cellulosic graft copolymers subjected to uniaxial stretching in film form. For intimately mixed multicomponent polymer systems such as random copolymers (Tagaya et al. 2006) and compatible polymer blends (Hahn and Wendorff 1985; Nishio et al. 1990; Nishio et al. 1994; Ohno and Nishio 2007; Yamaguchi and Masuzawa 2007), a noteworthy effect may be found in the optical properties of their oriented materials. That is, by adequately combining two ingredients that have opposite polarizability, the strain-induced birefringence can be voluntarily controlled, and, in a special case, the original optical isotropy is maintained regardless of the polymer chain orientation. Such a concept is

probably applicable to cellulosic graft copolymer systems. Besides, intercomponent miscibility is not a cause for concern to materialize intimate incorporations by graft copolymerization. Hardly any studies, however, have paid attention to the orientation behaviour correlated with molecular architectures for cellulosic graft copolymers.

In the present paper, we provide insight into the molecular orientation and optical anisotropy that are induced by the stretching of cellulose diacetate-*graft*-poly(L-lactide) (CDA-*g*-PLLA) in connection with the length of the grafted side-chains. To address the rigidity of the trunk polymers, flexible poly(vinyl acetate-*co*-vinyl alcohol) (P(VAc-*co*-VOH)) was also adopted as a trunk polymer, rather than semi-rigid cellulose diacetate (CDA). As is well known, not only cellulose acetate but also poly(vinyl alcohol) (PVOH) that is produced via saponification of poly(vinyl acetate) (PVAc) are both very important as film base for acting as optical devices to control the polarization state of light wave. For instance, in liquid crystal display (LCD) panels, PVOH is generally used as a basic component, polarizer, and triacetyl cellulose (TAC) is applied as a protection film of the polarizer (Nakayama et al. 2006). Birefringence of TAC films sometimes raises imperfect optical compensation on LCD, giving rise to a color shift of oblique incidence and/or a worse contrast of black/white level (Nakayama et al. 2006). Therefore, in the present study, there is an element of developing a way of controlling optical properties of these materials, especially for selection, regulation, or compensation of linearly polarized light.

The graft copolymers were synthesized by ring-opening copolymerization of L-lactide initiated at the residual hydroxyl groups of the trunk polymers in the presence of tin(II) 2-ethylhexanoate (Sn(II)Eht), which is known to be a highly selective catalyst (Kowalski et al. 1998). A fluorescence polarization technique

is employed to obtain information about the overall degree and type of molecular orientation developed in the drawing of graft copolymer films, while birefringence is used as a measure for estimation of the state of optical anisotropy of the drawn films.

Experimental Section

Original materials

CDA, kindly supplied by Daicel Chemical Industries Ltd., was determined as having a degree of substitution (DS) = 2.15 by ^{1}H NMR and number- and weight-average molecular weights (M_n and M_w) = 47.2 and 134 kg mol^{-1} by gel permeation chromatography (GPC) measurements. The procedures for the instrumental analyses will be described later. P(VAc-*co*-VOH) of a VAc/VOH composition of 64.2:35.8 in mol% was obtained as a solution in methyl acetate from General Science Corporation, Ltd. The composition was estimated through quantification of the carbon nuclei intensities of NMR using an inverse gated decoupling method (^{1}H-decoupled spectrum without NOE). The M_w (GPC) was 92.0 kg mol^{-1}. The as-provided P(VAc-*co*-VOH) solution was condensed once, dried at 40 °C *in vacuo*, and then dissolved in ethanol. The ethanol solution was added dropwise into an excess amount of distilled water with stirring. Purified P(VAc-*co*-VOH) as a precipitate was filtered, subjected to frost shattering for 3 min, and stored in a vacuum desiccator at 20 °C until used. To provide reference data of the orientation behaviour and optical isotropy, we also purchased PVOH (Nacalai Tesque Co.; nominal degree of polymerization, 500), PVAc

(Polysciences, Inc.; M_w, 900 kg mol^{-1}), and an additional copolymer sample P(VAc-*co*-VOH)# (Polysciences, Inc.; M_w, 720 kg mol^{-1}) with a molar ratio of VAc/VOH = 83.6/16.4. By means of quantitative ^{13}C NMR measurements according to the literature (Isasi et al. 1994; Tezuka et al. 1996), random distribution was confirmed for the acetyl groups on the anhydroglucose residue of CDA, and for the segments of VAc and VOH of the original P(VAc-*co*-VOH) used, as well.

L-Lactide was obtained from Purac Biochem and recrystallized from solution in dry toluene. Tin(II) 2-ethylhexanoate (Sn(II)Eht) catalyst and other organic solvents were purchased from Wako Pure Chemical Industries, Ltd. or Nacalai Tesque Co.; these were all guaranteed to be reagent-grade and used without further purification. A poly(L-lactide) (PLLA) homopolymer (LACTY, M_n (GPC) = 75.6 kg mol^{-1}) was kindly supplied by Shimadzu Co. Ltd. and used as received. The fluorescent molecule used as a probe for orientation estimation was a stilbene derivative, 4,4′-bis(2-benzoxazolyl)stilbene (BBS) (Sigma-Aldrich Co.), whose chemical structure is shown in Scheme 1.

Graft copolymerization

A trunk polymer, CDA (1.50 g; 5.04 mmol in hydroxyl groups) or P(VAc-*co*-VOH) (1.00 g; 5.04 mmol in hydroxyl groups), and L-lactide (4.00 g; 55.6 mmol in lactyl unit) were put into a flask and dried at 40 °C *in vacuo* for 12 h. Subsequently, 2, 10, or 20 mL of *N*,*N*-dimethylacetamide (DMAc) as a reaction solvent was added into the flask, which was then heated in an oil bath at 130 °C with stirring under a dried nitrogen atmosphere. After 20 min, the system became a transparent liquid, into which Sn(II)Eht (0.04 g, 0.196 mmol) was then

added. Continuous stirring was performed for a predetermined time. For the CDA series, the resultant polymeric product was dissolved in acetone and the homogeneous solution was added dropwise into a vigorously stirred, large excess of methanol or 2-propanol. For the P(VAc-*co*-VOH) series, on the other hand, the reaction mixture was diluted with dioxane, and the solution was reprecipitated in distilled water. After that, the crude product of grafted P(VAc-*co*-VOH) obtained as the reprecipitate was dissolved in chloroform and the solution was added dropwise into ice-chilled ethanol. Both grafted products, CDA-*g*-PLLA and P(VAc-*co*-VOH)-*g*-PLLA, were obtained finally as the reprecipitates, were filtered, dried in a vacuum oven regulated at 40 °C, and stored there until used.

Film preparation and stretching

A 5.0 wt% solution of each graft copolymer sample in DMF (CDA series) or in chloroform (P(VAc-*co*-VOH) series) was prepared at 20 °C. A small amount of BBS was dispersed into the respective copolymer solutions at a concentration of ~1.0×10^{-4} mol L^{-1}, at which level any effect of fluorescence depolarization, caused by energy migration due to the higher concentration of chromophores, becomes negligible (Nishio et al. 1994; Nishio et al. 1979). Graft copolymer films were cast from the solutions onto a glass plate through evaporation of DMF at 50 °C under reduced pressure (<10 mmHg) (CDA series) or through that of chloroform at 20 °C under ordinary pressure (P(VAc-*co*-VOH) series).

Strips (4 × 20 × ~0.1 mm in size) cut from the graft copolymer films were dried at 20 °C *in vacuo* for 3 days, followed by further heat treatment at 120 °C *in vacuo* for 10 min. Each of the film strips was fixed onto a hand-cranked drawing device which could be placed in a heated air oven. The film was then uniaxially

stretched to the desired draw ratio at the onset temperature of glass transition (as measured by differential scanning calorimetry, mentioned below) of the graft copolymer sample used. The deformation rate was ~45 mm min^{-1}. After completion of the drawing process, the film specimens were quickly cooled to 20 °C (CDA series) or 0 °C (P(VAc-*co*-VOH) series) and then stored in a desiccator at 20 °C until they were used for the orientation and birefringence measurements (see below). The draw ratio (λ) or percentage elongation (ε) [$\varepsilon = (\lambda - 1) \times 100$ %] of the oriented samples was determined from the positions of the ink marks on the film.

Measurements

300 MHz ^{1}H NMR spectra were recorded on a Varian INOVA 300 spectrometer using dimethylsulfoxide-d_6 (CDA series) or $CDCl_3$ (P(VAc-*co*-VOH) series) as a solvent. Figure 1 exemplifies ^{1}H NMR spectra obtained for selected samples of CDA-*g*-PLLA and P(VAc-*co*-VOH)-*g*-PLLA. The ^{1}H NMR data were used to determine the molecular compositions of the graft copolymers. For CDA-*g*-PLLA, the ordinary molar substitution (MS) can be estimated as the average number of introduced lactyl units per anhydroglucose residue of CDA. In the present study, however, a structural parameter OH-MS common to both graft copolymer series was mainly adopted to characterize the grafting degree, which was defined as the average number of introduced lactyl units per hydroxyl group of the original CDA or P(VAc-*co*-VOH) used as trunk. In addition, we specified %OH-substituted and DPs, respectively, as the percentage of substituted hydroxyl groups and as the average degree of polymerization of the PLLA side-chains.

In the ^{1}H NMR spectra of CDA-*g*-PLLA, if we designate a resonance peak area derived from the methyl protons of acetyl groups as **A**, an area of the resonance signals from the internal methyl protons of lactyls as **B**, and an area from the terminal methyl protons of lactyls as **C**, the MS, OH-MS, %OH-substituted, and DPs can be calculated by eqs. (1)–(4), respectively.

$$\text{MS} = 2.15 \times \{(\mathbf{B} + \mathbf{C}) / \mathbf{A}\} \quad (1)$$

$$\text{OH-MS} = 2.15 \times \{(\mathbf{B} + \mathbf{C}) / \mathbf{A}\} \times (1 / 0.85) \quad (2)$$

$$\%\text{OH-substituted} = 2.15 \times (\mathbf{C} / \mathbf{A}) \times (1 / 0.85) \times 100 \quad (3)$$

$$\text{DPs} = (\mathbf{B} + \mathbf{C}) / \mathbf{C} \quad (4)$$

where numerals 2.15 and 0.85 denote the acetyl DS and the number of residual hydroxyl groups per anhydroglucose unit, respectively, of the original CDA. For the other series P(VAc-*co*-VOH)-*g*-PLLA, if we designate a resonance peak area from the methyl protons of acetyl groups as **D**, an area of the resonance signals from the internal methine protons of lactyls as **E**, and an area from the terminal methine protons of lactyls as **F**, then

$$\text{OH-MS} = 0.642 \times \{(\mathbf{E} + \mathbf{F}) / (\mathbf{D} / 3)\} \times (1 / 0.358) \quad (5)$$

$$\%\text{OH-substituted} = 0.642 \times \{\mathbf{F} / (\mathbf{D} / 3)\} \times (1 / 0.358) \times 100 \quad (6)$$

$$\text{DPs} = (\mathbf{E} + \mathbf{F}) / \mathbf{F} \quad (7)$$

where numerals 0.642 and 0.358 indicate the molar fractions of the VAc and VOH units, respectively, in the trunk polymer. Accordingly, the PLLA weight content (w_{PLLA}) in the graft copolymer products can be calculated by using OH-MS, and the molecular weights of a repeating unit of the trunk polymer concerned and of a lactyl unit.

Quantitative ^{13}C NMR measurements were performed in a non-NOE gated decoupling technique (pulse repetition time, 30 s; scan number, 2000).

GPC was carried out at 40 °C using a Tosoh HLC-8020 equipped with a refractive index detector and two TSK-gel GMH_{HR}-H columns and calibrated with polystyrene standards. Tetrahydrofuran (THF) was used as an eluent at a flow rate of 0.5 mL min^{-1}. The concentration of test samples was 0.5 % in THF and the quantity of injection was 50 μL.

Differential scanning calorimetry (DSC) was conducted with a Seiko DSC6200/EXSTAR6000 apparatus. The measurements were carried out on 6–8-mg samples usually at a scanning rate of 20 °C min^{-1} under a nitrogen atmosphere, following calibration of the temperature readings with an indium standard. The samples were first cooled to −50 °C, heated to 250 °C (first heating scan), and then immediately quenched to −50 °C at a cooling rate of ~80 °C min^{-1}. The second heating scans were run from −50 °C to 250 °C. The thermal data reported in this paper were recorded during the second heating scan, which gave stable DSC traces.

Fluorescence polarization measurements were made at 20 °C using an apparatus that had been built in our laboratory (Nishio et al. 1994). When the alignment of the molecular axis (**M**-axis) of a florescent probe BBS (Scheme 1) is specified by a set of polar and azimuthal angles (ω, φ) in a sample coordinate system O-*XYZ*, where the *Z*- and *Y*-axes are aligned in the draw direction of a film sample and in a direction normal to the plane of the film surface, respectively, the molecular orientation state can be characterized statistically in terms of the second and fourth moments, as defined in the following way:

$$< \cos^k \omega >= \int_0^{2\pi} \int_0^{\pi} \cos^k \omega N(\omega, \varphi) \sin \omega \mathrm{d}\omega \mathrm{d}\varphi \quad (k = 2, 4) \qquad (8)$$

where $N(\omega, \varphi)$ is a normalized function that represents the molecular orientation distribution. According to a procedure previously established by Nishio et al.

(Nishio et al. 1994; Nishio et al. 1979), the values of $<\cos^2 \omega>$ and $<\cos^4 \omega>$ can be determined from equations 9 and 10, respectively.

$$<\cos^2 \omega>=\left[\left\{\frac{2(A^2+2)}{3A-1}\right\}\Big/\left\{2(A+2)-\frac{3I_{zz}-8I_{xx}}{I_{zz}+2I_{zx}}\right\}\right]+\frac{A-1}{3A-1} \qquad (9)$$

$$<\cos^4 \omega>=\frac{4}{(3A-1)^2}\left\{\frac{A(3A-1)}{2}<\cos^2 \omega>-\frac{A^2-1}{4}-\frac{(3A-1)<\cos^2 \omega>-(A-1)}{(I_{zz}/I_{zx}+2)}\right\} \qquad (10)$$

where I_{ij} ($i, j = X$ or Z) is a polarized component of the fluorescence intensity, and A is a parameter that characterizes the intrinsic photophysical anisotropy of the fluorescent molecule which is dispersed as an orientation probe in a polymeric medium. Four polarized components - I_{zz}, I_{zx}, I_{xx}, and I_{xz} - were measured using the following combinations of the transmission axis of a polarizer and that of an analyzer: let I_{zz} be a polarized component of the fluorescence intensity that is observed when the two axes are both parallel to the Z-axis, and let I_{zx} be the component obtained when the axis of the polarizer and that of the analyzer are parallel to the Z- and X- axes, respectively. I_{xx} and I_{xz} can be defined in a similar way. For the stilbene derivative BBS, the anisotropy of light absorption and that of emission were assumed to be similar in extent, since the observed intensities I_{zx} and I_{xz} were almost equal to each other, irrespective of the degree of orientation of the actually drawn samples (Nishio et al. 1994). The value of A can then be obtained from the following relationship that is applicable to undrawn samples with a random orientation distribution:

$$\frac{I_{zz}-I_{zx}}{I_{zz}+2I_{zx}}=\frac{2}{5}\left(\frac{3A-1}{2}\right)^2 \qquad (11)$$

Ideally, the A value is 1, if both the light-absorbing and the light-emitting axes of the fluorescent probe coincide with the molecular axis **M** to become a single linear oscillator. Actually however, the value is usually less than 1 due to some

effects involving thermal fluctuation in the structure of the molecule. In the present study, an average data $A = 0.86$ estimated for undrawn films was used for calculating the moments of molecular orientation.

The birefringence (Δn) of drawn graft copolymer samples was determined using an Olympus BX60F5 polarized optical microscope with a Berek compensator, at 20 °C. Throughout this work, Δn is defined as the difference, $\Delta n = n_{\parallel} - n_{\perp}$, between a refractive index ($n_{\parallel}$) parallel to the draw direction and that ($n_{\perp}$) perpendicular to it.

Results and Discussion

Synthesis of Graft Copolymers

Figure 2 illustrates a result of the monitoring OH-MS, %OH-substituted, and DPs for the two graft copolymerization systems as a function of time. Even though data of the time-course of OH-MS for the two systems were comparable to each other (Fig. 2a), %OH-substituted and DPs were higher and lower, respectively, in the CDA series. Such a different behaviour upon the introduction of graft chains may be attributed to a conformational difference between the two trunk polymers; viz., the efficiency of Sn(II)Eht catalyst coordination is presumed to be higher for the semi-rigid CDA trunk chain due to less steric interference in solution, rather than the situation for the flexible chain of P(VAc-*co*-VOH). However, once the graft segment is introduced onto the P(VAc-*co*-VOH) backbone, the terminal would be easily acceptable for the catalyst to access again, so that the chain

propagation progresses advantageously; thus, the increment of DPs was larger for this trunk polymer than that for the CDA backbone.

Table 1 summarizes various molecular parameters determined for the copolymer samples provided for the drawing experiment, together with conditions of the graft reaction. As has been described in our previous papers (Teramoto and Nishio 2003; Teramoto et al. 2004), the reaction solvent (DMAc) was apt to suppress the reactivity of the L-lactide monomer for the ring-opening graft copolymerization; in fact, a higher degree of grafting was accomplished when the addition of solvent was decreased. Thus, the two graft copolymer series were prepared successfully for a wide range of compositions.

Thermal Transition Behaviour of Graft Copolymers

Figure 3 illustrates DSC data obtained for selected samples of the two graft copolymer series, where arrows indicate an onset glass transition temperature T_g corresponding to the processing temperature for film stretching in the present work. The thermal transition behaviour of the series of CDA-*g*-PLLA has already been described in detail in a previous paper (Teramoto and Nishio 2003): the T_g (mid-point) decreased sharply from 202 °C of the original CDA to ~50 °C with increasing MS up to ~12 and converged a little under a mid-point T_g (62 °C) of PLLA homopolymer with a further increase in MS. When the MS reached or exceeded 14, as-prepared graft copolymers exhibited a crystalline phase of PLLA side-chains. All the CDA-*g*-PLLA samples investigated in this work showed a single glass transition and a continuous depression of the T_g with increasing side-chain content. As has been reported earlier, no phase separation occurs in the amorphous CDA-*g*-PLLA materials, at least on the scale of T_g-detection, which is

usually assumed to be less than a couple of tens of nanometers (Kaplan 1976; Nishio 1994; Utracki 1990).

For the P(VAc-*co*-VOH)-*g*-PLLA series, no great T_g variation was observed in comparison with the case of the CDA series. This is primarily because this combination of the trunk and graft exhibits closely situated T_gs. However, as shown in the insert of Figure 3b, the onset T_g decreased gently from 52 °C of the original P(VAc-*co*-VOH) to 45 °C with increasing OH-MS up to 1.72. The lowering action of T_g is attributable to less degree of intermolecular interaction such as hydrogen bonding between trunk polymers, due to the grafting of PLLA (oligomer). With a further increase in the side-chain content, there occurs a T_g elevation of the grafting PLLA itself with prominence of the high-polymeric nature. Eventually, it is possible to interpret the composition dependence of T_g for the P(VAc-*co*-VOH)-*g*-PLLA in the similar manner for the CDA series, and to assume that no phase separation occurs in this series of copolymer. In addition, the thermograms exhibited a small single endotherm overlapping the glass transition, due to excess-enthalpy relaxation as a result of the physical aging in the DSC scans (Weitz and Wunderlich 1974). The single relaxation signal is a collateral evidence for no occurrence of phase separation in the amorphous P(VAc-*co*-VOH)-*g*-PLLA.

On the other hand, crystalline development was not observed for either of the graft copolymer series. This absence is regarded as reasonable because (1) the P(VAc-*co*-VOH) used here has no crystallizability, (2) a potential crystallizability of the original CDA (when heat treated) was diminished by the incorporation of the grafts, and (3) the lengths of the side-chains introduced here were not long enough to form PLLA crystals. Thus, all the graft copolymers investigated here are considered to be non-crystallizable and to be intimately combined by each set

of the two components that constitute the copolymers, without any domain segregation.

Molecular Orientation

In Figure 4, the second moment of molecular orientation, $\langle \cos^2 \omega \rangle$, evaluated by the fluorescence polarization method, is plotted against the percentage elongation of film specimens of CDA, CDA-*g*-PLLA, P(VAc-*co*-VOH), P(VAc-*co*-VOH)-*g*-PLLA, and PLLA. For comparison, the data for PVOH, PVAc, and P(VAc-*co*-VOH)# are also included in Figure 4a. For all the film samples, we find that the value of $\langle \cos^2 \omega \rangle$ increases monotonically from 0.333 with increasing extent of elongation, irrespective of the chemical composition of the polymer medium used. Therefore it follows that the drawn films gave a definitely "positive" orientation function, i.e., $f = (3\langle \cos^2 \omega \rangle - 1)/2 > 0$, which indicates a "normal" trend for molecular orientation in the draw direction.

A broken line in the respective parts a–c of Figure 4 represents a theoretical curve according to the Kratky-type affine transformation scheme (Kratky 1933), proposed for the orientation of rodlike structural units floating in a bulk matrix. In this scheme, when the bulk is deformed uniaxially at a draw ratio λ, the orientation distribution of the rods obeys the following function:

$$N(\omega, \varphi) = \frac{1}{4\pi} \times \frac{n^2}{(n^2 \sin^2 \omega + \cos^2 \omega)^{3/2}} \qquad (12a)$$

$$\text{with } n = (\lambda)^{3/2} \qquad (12b)$$

As exemplified in Figure 4a and b, the film of unmodified CDA showed a high level of molecular orientation upon stretching, so as to make a just fit of the $\langle \cos^2 \omega \rangle$ vs. percent elongation plot to the theoretical curve of the affine

deformation; however, the film specimen was prone to break at an earlier stage of elongation (ε = ~50 %). The capability of CDA to assume such a high orientational action may be attributed not only to its semi-rigid carbohydrate backbone, but also partly to the intermolecular interaction via hydrogen-bonding between the residual hydroxyl groups (Ohno and Nishio 2007).

A high degree of molecular orientation was also observed for PVOH homopolymer capable of forming a well-developed hydrogen-bonding network in the film material. As shown in Figure 4a, the plot of $\langle\cos^2\omega\rangle$ values against percent elongation fitted the theoretical curve assuming the affine deformation at the elongation stage of $\varepsilon \leq 50$ %, and the molecular orientation at higher elongations even exceeded the orientation predicted by the deformation model. In the partially acetylated form, however, a lower level of orientation prevailed in the drawn films, this situation being pronounced with a decrease in molar fraction of the interactive VOH unit, as can be seen from Figure 4a. Especially, the VAc-rich P(VAc-*co*-VOH)# and PVAc samples were highly susceptible to plastic flow during deformation at T_g and higher temperatures; a rapid orientation relaxation concurrent with the drawing process may be responsible for their inherently lower extent of capability for orientation.

Concerning the two graft series (Figure 4b and c), the $\langle\cos^2\omega\rangle$ vs. percent elongation plots for all the copolymer compositions were located below the corresponding plot obtained for the respective trunk polymers *per se*, CDA and P(VAc-*co*-VOH). Comparing the overall degree of molecular orientation between the two series, the CDA-*g*-PLLA series of semi-rigid backbone was superior to the P(VAc-*co*-VOH)-*g*-PLLA series, as far as films specimens were deformed within the elongation limits of $\varepsilon \leq 50$ % above which the former series showed a habit of breaking. In connection with discussion to be given later, it

should be stressed here that, in any of the two series, the degree of orientation decreased monotonically with an increase in OH-MS, when compared at a given stage of elongation. In the drawing of the copolymer samples, deservedly, the tensile stress was applied not only onto the trunk polymer chains but also onto the attached side-chains. It is then plausible to assume that the stress component distributed to the side-chains less contributed to the molecular orientation in the draw direction. In addition to this presumption, presumably, the higher the OH-MS, the lower the density of supporting points such as hydrogen bonding and/or entanglement between the trunk polymers should be. Accordingly, the molecular mobility as a whole of the graft copolymer concerned is so enhanced that the orientation relaxation would be noticeable in the drawing process.

Using the fluorescence polarization technique, it is possible to obtain information about not only the degree but also the type of molecular orientation in the non-crystalline regions of polymer solids (Nishio et al. 1994; Nishio et al. 1979; Nishijima 1970). A convenient method for estimating the type of molecular orientation is to construct a plot of the fourth moment against the second moment of orientation, and to then search for conformity of the plot to the relationship between the moments calculated in terms of some potential model of the orientation distribution. Examples of the construction of the $\langle \cos^4 \omega \rangle$ vs. $\langle \cos^2 \omega \rangle$ plot are shown in Figure 5 for selected compositions of the graft copolymers CDA-*g*-PLLA (Figure 5a) and P(VAc-*co*-VOH)-*g*-PLLA (Figure 5b), with the films being deformed to a percentage of 20 ± 5 % for the CDA series and 135 ± 15 % for the P(VAc-*co*-VOH)-*g*-PLLA series. It can be seen that the position of the data points in the plots for both series shifts progressively toward the lower and left side with increasing OH-MS. A continuous line in the respective figures represents a relationship derived by assuming that the molecular

orientation distribution obeys a type of prolate ellipsoid of rotation around the stretching axis. The calculated curve is virtually equivalent to a theoretical curve predicted by the Kratky-type affine deformation scheme, if the parameter *n* in equation 12a is taken to be a variable axial ratio of the ellipsoid. As demonstrated in the figures, the experimental data obtained for all drawn films of the two series fitted the calculated curve, which implies that the type of molecular orientation distribution in the uniaxially deformed copolymer films follows well the ellipsoidal model, regardless of the rate of orientation development.

Optical Anisotropy

Optical birefringence derives from the orientation of polymer chains that inherently have the anisotropy of polarizability. In the simplest case of uniaxial stretching of amorphous homopolymers, the extent of birefringence Δn ($= n_{\parallel} - n_{\perp}$) varies monotonically with the degree of orientation, irrespective of whether Δn° is positive or negative, according to the equation:

$$\Delta n = \frac{1}{2}(3 < \cos^2 \omega_S > -1)\Delta n^{\circ} \qquad (13)$$

where Δn° is the intrinsic birefringence for the perfect uniaxial orientation of polymer chains, and $<\cos^2 \omega_S>$ is the second moment of orientation for an anisotropic segmental unit **S** with a certain polarizability. Here it should be noted that the two second moments, $<\cos^2 \omega>$ and $<\cos^2 \omega_S>$, obtained from the fluorescence polarization and birefringence measurements, respectively, are generally different in magnitude from each other, since there should be a respectable difference in size of the structural unit for orientation estimation between the two methods (usually $|\mathbf{S}| < |\mathbf{M}|$).

Figure 6 compiles data of the birefringence measurements carried out on drawn films of the two series of graft copolymers (parts b and c) and the component polymers and related ones (part a). As is already known (Ohno and Nishio 2007; Sata et al. 2004), cellulose acetates of DS = 1.8–2.7, including the present CDA of DS = 2.15, exhibit positive optical anisotropy ($\Delta n > 0$) upon stretching. It is also informed that the rise of Δn with percentage elongation was noticeably suppressed with increasing DS, and drawn cellulose triacetates of DS > 2.8 showed negative optical anisotropy. The observations are interpretable by assuming that the acetyl carbonyl groups would be aligned almost perpendicular to the cellulose backbone and behave so as to compensate for the positive anisotropy of the normally oriented trunk polymer chain.

The vinyl homopolymer PVOH showed positive optical anisotropy upon stretching and the value of Δn increased remarkably with increasing elongation, whereas the fully acetylated form PVAc provided a definitely negative birefringence. Values of Δn observed for the partially acetylated forms, P(VAc-*co*-VOH) and P(VAc-*co*-VOH)#, were also negative and generally diminished with the increase in the degree of acetylation. As shown in Figure 6a, however, the Δn vs. percent elongation plot for P(VAc-*co*-VOH)# was located in close proximity to the position of the corresponding plot for PVAc homopolymer. The development of molecular orientation was comparatively better in dawn films of the former polymer (Figure 4a); probably this resulted in a rather greater contribution of the VAc unit to the negative birefringence. As can also be seen from Figure 6a, drawn films of the aliphatic polyester PLLA exhibited quite a high level of optical anisotropy of $\Delta n > 0$, the level surpassing that for drawn PVOH films that showed a higher degree of orientation rather than the PLLA films (Figure 4a). It is therefore suggested that the intrinsic anisotropy in

polarizability of a statistical PLLA-chain segment is considerably higher compared with the situation in PVOH.

Figure 7 schematically explains the orientational birefringence in the two series of graft copolymers. Schemes in the uppermost row in the figure represent the anisotropy in polarizability units belonging to the respective component polymers, CDA, PVOH, PVAc, and PLLA. Parts a–d and e–h of Figure 7 depict schematic models of oriented molecular chains for the elongated CDA-*g*-PLLA and P(VAc-*co*-VOH)-*g*-PLLA series, respectively, with different lengths of the PLLA graft chain. For the sake of convenience, all the polymer chains are illustrated as a sequence of the polarizability ellipsoids of the constituent monomeric units, although such a polarizability ellipsoid is not necessarily related to a single monomeric unit. The relative dimensions of the principal axes of each individual polarizability ellipsoid qualitatively reflect the intrinsic refractive indices ($n_{\parallel}°$ and $n_{\perp}°$) in the relevant chain segment.

In Figure 6b and c, plots of Δn vs. percentage elongation are constructed for a wide range of compositions of the two series of graft copolymers. Obviously, all the CDA-graft copolymers exhibited positive optical anisotropy ($\Delta n > 0$) upon stretching (Figure 6b), while the drawn P(VAc-*co*-VOH)-*g*-PLLA films imparted a negative birefringence (Figure 6c). These polarities, opposite to each other between the two series, seem to insistently reflect the original birefringence of the respective trunk polymers. The optical anisotropy of the P(VAc-*co*-VOH)-*g*-PLLA films induced by stretching was relatively low, which can be attributed primarily to the prevalence of a lower degree of orientation of the polymer molecules in the stretched samples, as supported by the result of the fluorescence polarization measurements (Figure 4c).

As a consequence of the grafting with PLLA (oligomer), roughly, absolute values of Δn were lowered in both the elongated CDA and P(VAc-*co*-VOH) series. This can also be interpreted as being basically due to the development of lower degrees of molecular orientation in the graft copolymer films. Through careful observations, however, we find an interesting discontinuous change in location level of the Δn vs. percentage elongation plot, with the varying OH-MS parameter proportional to the graft-chain length. Reasonable explanations for the birefringence behaviour are given as follows.

(A) CDA-*g*-PLLA series:

i) As to the samples of low OH-MSs (0.44 and 0.75) less than 1.0, the trunk CDA chains tend to better align parallel to the draw direction, but, at the same time, the lactyl units attached onto the cellulose backbone are arranged with the longer principal axis of polarizability perpendicular to the draw direction, as illustrated in Figure 7b. This lactyl arrangement would make a rather large negative contribution to the total birefringence.

ii) With a modest increase in OH-MS, e.g., to 1.29, the lactyl units apart from the joint of PLLA-grafting could orient in the draw direction, as shown diagrammatically in Figure 7c. This should make a positive contribution to the total birefringence. Actually, the plot of Δn vs. percent elongation obtained for the copolymer of OH-MS = 1.29 is located above the corresponding plots for the ones of OH-MS = 0.44 and 0.75 (Figure 6b); on the contrary, the former sample is inferior in the level of overall molecular orientation to the latter ones (Figure 4b).

iii) A further increase in OH-MS, e.g., to 3.33 would give rise to a lower degree of orientation of the entire copolymer molecule having flexible, longer graft chains (Figure 7d), which may be approved by the $<\cos^2\omega>$ estimation shown

in Figure 4b. This results in serious suppression in the rise of the Δn vs. percent elongation curve (Figure 6b).

(B) P(VAc-*co*-VOH)-*g*-PLLA series:

iv) As to the samples of low OH-MSs (0.64 and 0.93), the lactyl units introduced in a small fragment would exhibit a tendency to be collocated perpendicular to the trunk vinyl polymer (Figure 7f), as does in the case of the CDA series of OH-MS < 1.0. Such lactyl units behave as a negative anisotropic unit of polarizability when the trunk chain is oriented in the draw direction, so as to decrease Δn (i.e., to enhance the absolute value), as seen in Figure 6c.

v) When the substitution parameter OH-MS reaches 1.72, some lactyl groups apart from the graft joint would be arranged parallel to the draw direction (Figure 7g) and hence serve as a positive anisotropic unit of polarizability. The positive contribution should compensate the negative one of the lactyl units connected directly to the vinyl alcohol segments. Thus we see the reason for the location of the Δn vs. percent elongation plot for the graft copolymer of OH-MS = 1.72 at a little higher level relative to the plot for ungrafted P(VAc-*co*-VOH).

vi) As to the compositions of still higher OH-MSs (>2.0), Δn increases (the absolute value decreases) more and more with the variation of OH-MS from 2.04 to 10.4 through 5.26 (Figure 6c). This change may be ascribed to the essentially lower level of orientation of the entire graft copolymer molecules in the drawn samples, as well as to the partly positive contribution of the longer PLLA side-chains to the total birefringence (Figure 7h).

Conclusions

CDA-*g*-PLLA and P(VAc-*co*-VOH)-*g*-PLLA were successfully prepared over a range of compositions of the respective trunk/graft pairs, by ring-opening copolymerization of L-lactide at the residual hydroxyl positions of CDA (acetyl DS = 2.15) and P(VAc-*co*-VOH) (VAc = 64.2 mol%). Both series of graft copolymers synthesized were totally non-crystalline and their solution-cast films were regarded as intimately incorporated composite showing no phase separation of the trunk and side-chain components.

The molecular orientation and optical anisotropy induced by uniaxial stretching of film specimens were investigated for the above two series by techniques of fluorescence polarization and birefringence measurements. In the former technique, a fluorescent stilbene derivative BBS of ~2.5 nm length was utilized as a probe for estimating the overall molecular orientation behaviour in the dawn films. Upon stretching, any film of both series imparted a positive orientation function, i.e., $f = (3\langle\cos^2\omega\rangle - 1)/2 > 0$, which increased with the extent of elongation. The degree of molecular orientation was generally higher in the CDA-graft series with a semi-rigid trunk, although the deformability of this series was smaller relative to that of the P(VAc-*co*-VOH)-graft series. In both series, the orientation development was declined monotonically with increasing content of the PLLA side-chain component. It was also deduced from the $\langle\cos^4\omega\rangle$ vs. $\langle\cos^2\omega\rangle$ relationship that the type of statistical orientation distribution followed an orthodox, prolate ellipsoidal model, irrespective the copolymer composition as well as of the sort of the trunk polymer used.

The two polymers used as trunk, CDA and P(VAc-*co*-VOH), showed mutually opposite signs in the intrinsic birefringence, and the drawing of the respective graft copolymer films provided the orientation-induced birefringence

changeable in a certain range of values depending on the OH-MS parameter proportional to the PLLA-chain length. CDA-*g*-PLLA films exhibited positive optical anisotropy ($\Delta n > 0$) upon stretching, while P(VAc-*co*-VOH)-*g*-PLLA drawn films displayed negative one; this contrast in polarity substantially reflects the difference in the original birefringence between the trunk polymers. However, for both graft series, we observed a non-monotonic change in location level of the Δn vs. percent elongation plot, with varying OH-MS. The observation was explicable by assuming the locally different orientation manners of the attached PLLA chain-segments; viz., the lactyl units placed in close proximity to the graft joint would be arranged perpendicular to the trunk chain that is mainly aligned in the draw direction, whereas the lactyl units apart from the joint would orient preferably in the draw direction. The former situation makes a negative contribution and the latter does a positive contribution to the total birefringence.

The magnitude and even polarity of the intrinsic birefringences of cellulose acetate and P(VAc-*co*-VOH) are changeable by altering the content of the acetyl moiety. Therefore, this kind of graft copolymerization with another elaborate design of the trunk/graft combination ensures not only a more wide-ranging control but also a very subtle alteration in the optical property of polymeric bulk materials.

References

Hahn BR, Wendorff JH (1985) Compensation method for zero birefringence in oriented polymers. Polymer 26:1619-1622

Isasi JR, Cesteros LC, Katime I (1994) Hydrogen bonding and sequence distribution in poly(vinyl acetate-*co*-vinyl alcohol) copolymers. Macromolecules 27:2200-2205

Kaplan DS (1976) Structure-property relationships in copolymers to composites: Molecular interpretations of the glass transition phenomemon. J Appl Polym Sci 20:2615-2629

Kowalski A, Duda A, Penczek S (1998) Kinetics and mechanism of cyclic esters polymerization initiated with tin(II) octoate, 1. Polymerization of ε-caprolactone. Macromol Rapid Commun 19:567-572

Kratky O (1933) Deformation of cellulose films. Kolloid Z 64:213-222

Kusumi R, Lee SH, Teramoto Y, Nishio Y (2009) Cellulose ester-*graft*-poly(ε-caprolactone): Effects of copolymer composition and intercomponent miscibility on the enzymatic hydrolysis behavior. Biomacromolecules 10:2830-2838

Kusumi R, Teramoto Y, Nishio Y (2008) Crystallization behavior of poly(ε-caprolactone) grafted onto cellulose alkyl esters: Effects of copolymer composition and intercomponent miscibility. Macromol Chem Phys 209:2135-2146

Nakayama H, Fukagawa N, Nishiura Y, Yasuda T, Ito T, Mihayashi K (2006) Development of low-retardation TAC film for protection films of LCD's polarizer. J Photopolym Sci Technol 19:169-173

Nishijima Y (1970) Fluorescence methods in polymer science. J Polym Sci: Part C 31:353-373

Nishio Y (1994) Hyperfine composites of cellulose with synthetic polymers. In: Gilbert RD (ed) Cellulose polymers, blends, and composites. Hanser, Munich, New York, pp 95-113

Nishio Y (2006) Material functionalization of cellulose and related polysaccharides via diverse microcompositions. Adv Polym Sci 205:97-151

Nishio Y, Haratani T, Takahashi T (1990) Miscibility and orientation behavior of poly(vinyl alcohol)/poly(vinyl pyrrolidone) blends. J Polym Sci, Polym Phys Ed 28:355-376

Nishio Y, Suzuki H, Sato K (1994) Molecular orientation and optical anisotropy induced by the stretching of poly(vinyl alcohol)/poly(*N*-vinyl pyrrolidone) blends. Polymer 35:1452-1461

Nishio Y, Tanaka H, Onogi Y, Nishijima Y (1979) General analysis of fluorescence polarization in the anisotropic system (II) Experimental verification for the case of uniaxially oriented polymer films. Repts Progr Polym Phys Jpn 22:469-472

Ohno T, Nishio Y (2007) Molecular orientation and optical anisotropy in drawn films of miscible blends composed of cellulose acetate and poly(*N*-vinylpyrrolidone-*co*-methyl methacrylate). Macromolecules 40:3468-3476

Sata H, Murayama M, Shimamoto S (2004) Properties and applications of cellulose triacetate film. Macromol Symp 208:323-334

Tagaya A, Ohkita H, Harada T, Ishibashi K, Koike Y (2006) Zero-birefringence optical polymers. Macromolecules 39:3019-3023

Teramoto Y, Ama S, Higeshiro T, Nishio Y (2004) Cellulose acetate-*graft*-poly(hydroxyalkanoate)s: Synthesis and dependence of the thermal properties on copolymer composition. Macromol Chem Phys 205:1904-1915

Teramoto Y, Nishio Y (2003) Cellulose diacetate-*graft*-poly(lactic acid)s: Synthesis of wide-ranging compositions and their thermal and mechanical properties. Polymer 44:2701-2709

Teramoto Y, Nishio Y (2004a) Biodegradable cellulose diacetate-*graft*-poly(L-lactide)s: Enzymatic hydrolysis behavior and surface morphological characterization. Biomacromolecules 5:407-414

Teramoto Y, Nishio Y (2004b) Biodegradable cellulose diacetate-*graft*-poly(L-lactide)s: Thermal treatment effect on the development of supramolecular structures. Biomacromolecules 5:397-406

Tezuka Y, Tsuchiya Y, Shiomi T (1996) ^{13}C NMR determination of substituent distribution in carboxymethylcellulose by use of its peresterified derivatives. Carbohydr Res 291:99-108

Utracki LA (1990) Polymer alloys and blends. Hanser Gardner Publications, Munich

Weitz A, Wunderlich B (1974) Thermal analysis and dilatometry of glasses formed under elevated pressure. J Polym Sci: Polym Phys Ed 12:2473-2491

Yamaguchi M, Masuzawa K (2007) Birefringence control for binary blends of cellulose acetate propionate and poly(vinyl acetate). Eur Polym J 43:3277-3282

Figure Legends

Scheme 1 Structural formula of BBS.

Figure 1 ^{1}H NMR spectra of (a) CDA-*g*-PLLA with OH-MS = 3.33 and (b) P(VAc-*co*-VOH)-*g*-PLLA with OH-MS = 5.26.

Figure 2 Time-course of (a) OH-MS, (b) %OH-substituted, and (c) DPs for CDA-*g*-PLLA and P(VAc-*co*-VOH)-*g*-PLLA samples synthesized by ring-opening graft copolymerization of L-lactide onto the respective trunk polymers in DMAc (10 mL).

Figure 3 DSC thermograms (second heating scan) obtained for (a) CDA-*g*-PLLA and (b) P(VAc-*co*-VOH)-*g*-PLLA. Arrows indicate a T_g position taken as the onset of a baseline shift. Numerals denote OH-MS values for the graft copolymers.

Figure 4 Plots of $\langle\cos^2\omega\rangle$ vs. % elongation for film samples of the two series of graft copolymers, CDA-*g*-PLLA (part b) and P(VAc-*co*-VOH)-*g*-PLLA (part c), and of their component polymers and related ones (part a). A broken line represents a theoretical curve according to the Kratky-type affine deformation model. Numerals inserted in parts b and c denote OH-MS values for the graft copolymers.

Figure 5 $\langle\cos^4\omega\rangle$ vs. $\langle\cos^2\omega\rangle$ plots for (a) CDA-*g*-PLLA films elongated at ε = 16–25 % and (b) P(VAc-*co*-VOH)-*g*-PLLA films elongated at ε = 120–150 %. The continuous lines represent a relationship between the two moments calculated in terms of a model of a prolate ellipsoid of rotation for the type of molecular orientation distribution. Numerals put outside parentheses (% elongation) in the inserts denote OH-MS values.

Figure 6 Plots of birefringence vs. % elongation for film samples of the two series of graft copolymers, CDA-*g*-PLLA (part b) and P(VAc-*co*-VOH)-*g*-PLLA (part c), and of their component polymers and related ones (part a). Numerals inserted in parts b and c denote OH-MS values for the graft copolymers.

Figure 7 Schematic representation of orientational birefringence in CDA-*g*-PLLA (a–d) and P(VAc-*co*-VOH)-*g*-PLLA (e–h). Polymeric chains are illustrated as a sequence of the polarizability ellipsoids of the constituent monomeric units.

Table 1 Preparation Conditions and Molecular Parameters for Major Graft Copolymer Products

Reaction time /min	Solvent (DMAc) addition/mL	M_n[a] /kg mol^{-1}	M_w[a] /kg mol^{-1}	OH-MS[b]	MS[b]	%OH-substituted[b]	DPs[b]	w_{PLLA}[b]
CDA-*g*-PLLA series								
10	20	73.4	123	0.44	0.38	19.9	2.21	0.095
30	20	91.0	159	0.75	0.64	33.8	2.22	0.155
60	20	97.1	224	1.29	1.10	39.8	3.24	0.239
60	2	99.2	240	3.33	2.83	64.9	5.13	0.447
P(VAc-*co*-VOH)-*g*-PLLA series								
10	20	42.2	94.8	0.64	-	19.8	3.23	0.189
40	20	42.3	96.1	0.93	-	26.2	3.55	0.253
90	20	70.8	175	1.72	-	37.2	4.62	0.385
120	20	75.0	186	2.04	-	40.8	5.00	0.426
300	20	79.3	176	5.26	-	59.2	8.89	0.656
60	2	130	278	10.4	-	63.7	16.3	0.791

[a] Determined by GPC.

[b] Estimated from ^{1}H NMR spectra.

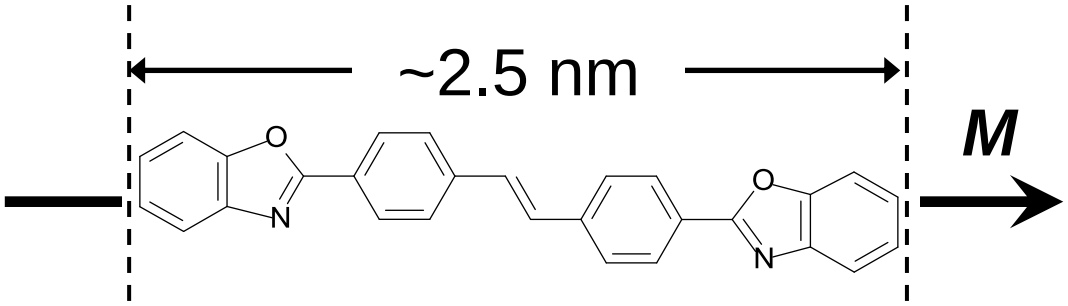

Scheme 1

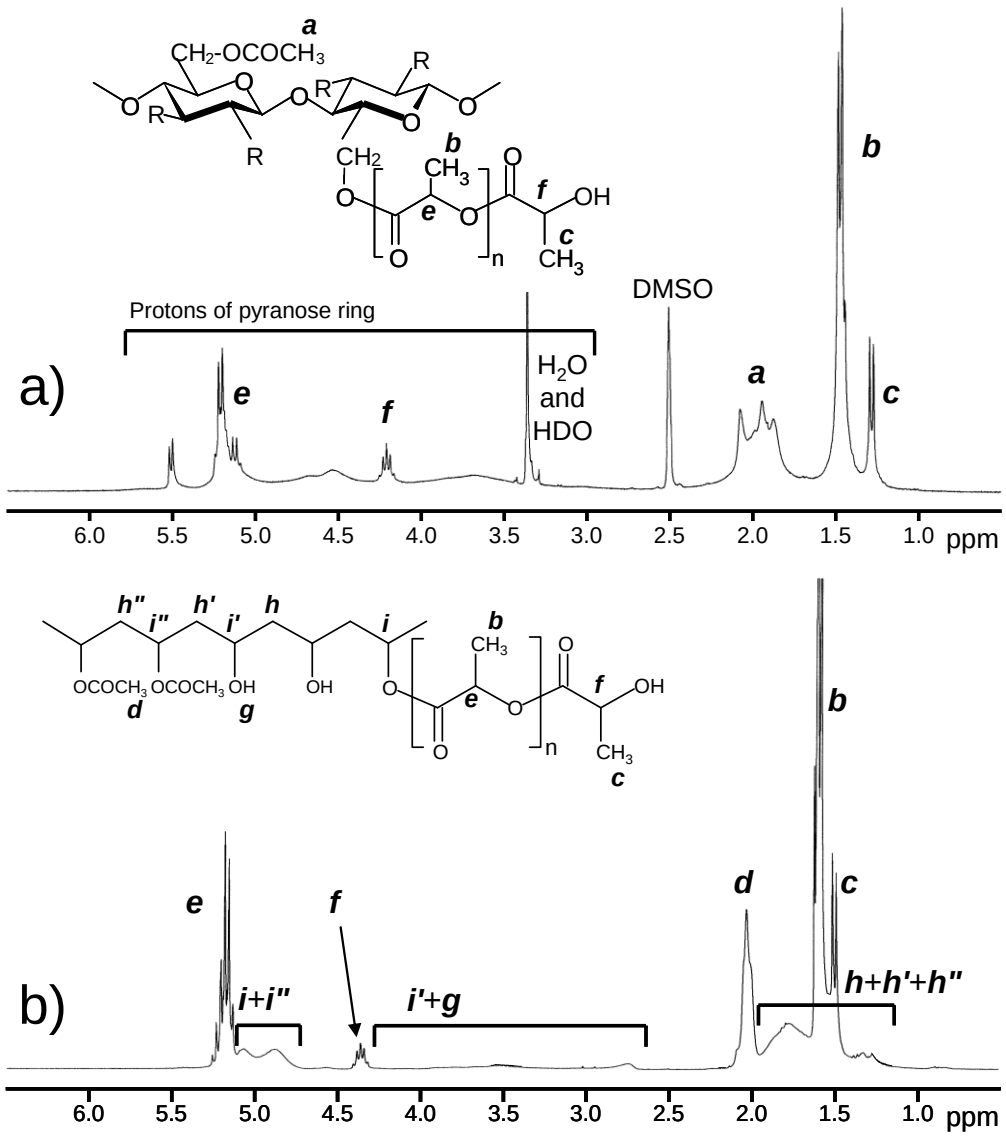
a
CH2-OCOCH3
R
O
b
CH2
CH3
f
OH
e
c
n
Protons of pyranose ring
DMSO
H2O
and
HDO
a)
6.0
5.5
5.0
4.5
4.0
3.5
3.0
2.5
2.0
1.5
1.0
ppm
h"
i"
h'
i'
h
i
OCOCH3
OH
d
g
b)
e
f
d
c
i+i"
i'+g
h+h'+h"

Figure 1

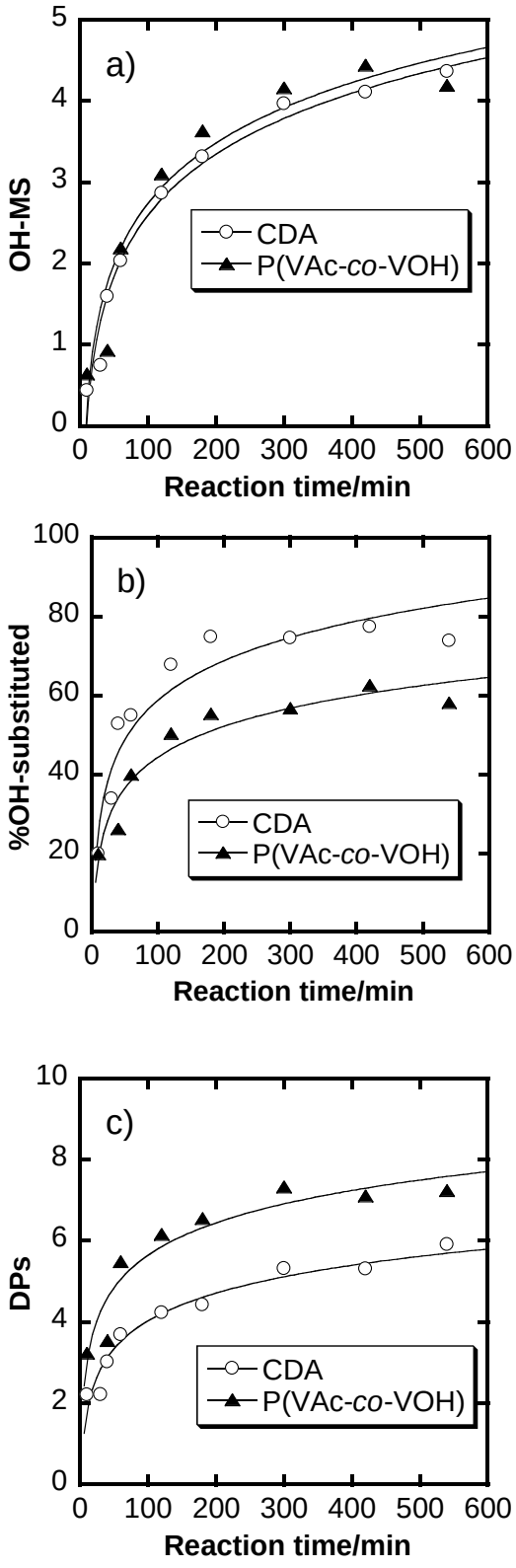
a)
OH-MS
Reaction time/min
CDA
P(VAc-co-VOH)
b)
%OH-substituted
Reaction time/min
CDA
P(VAc-co-VOH)
c)
DPs
Reaction time/min
CDA
P(VAc-co-VOH)

Figure 2

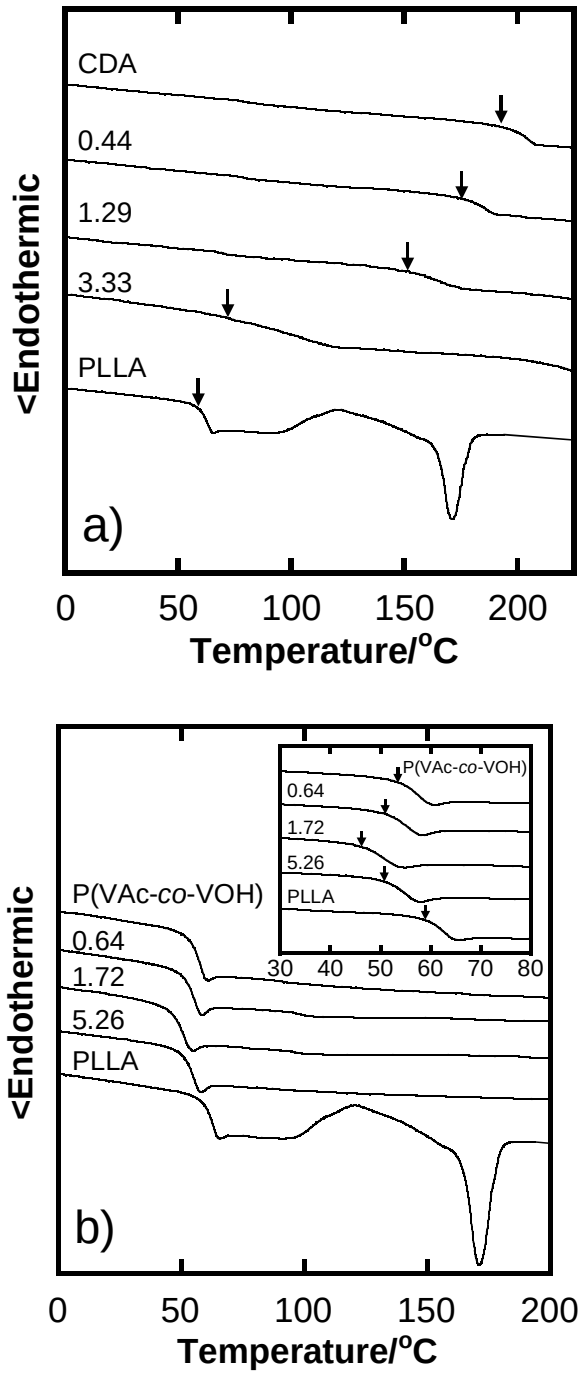
CDA
0.44
1.29
3.33
PLLA
a)
<Endothermic
0
50
100
150
200
Temperature/°C
P(VAc-co-VOH)
0.64
1.72
5.26
PLLA
30
40
50
60
70
80
b)

Figure 3

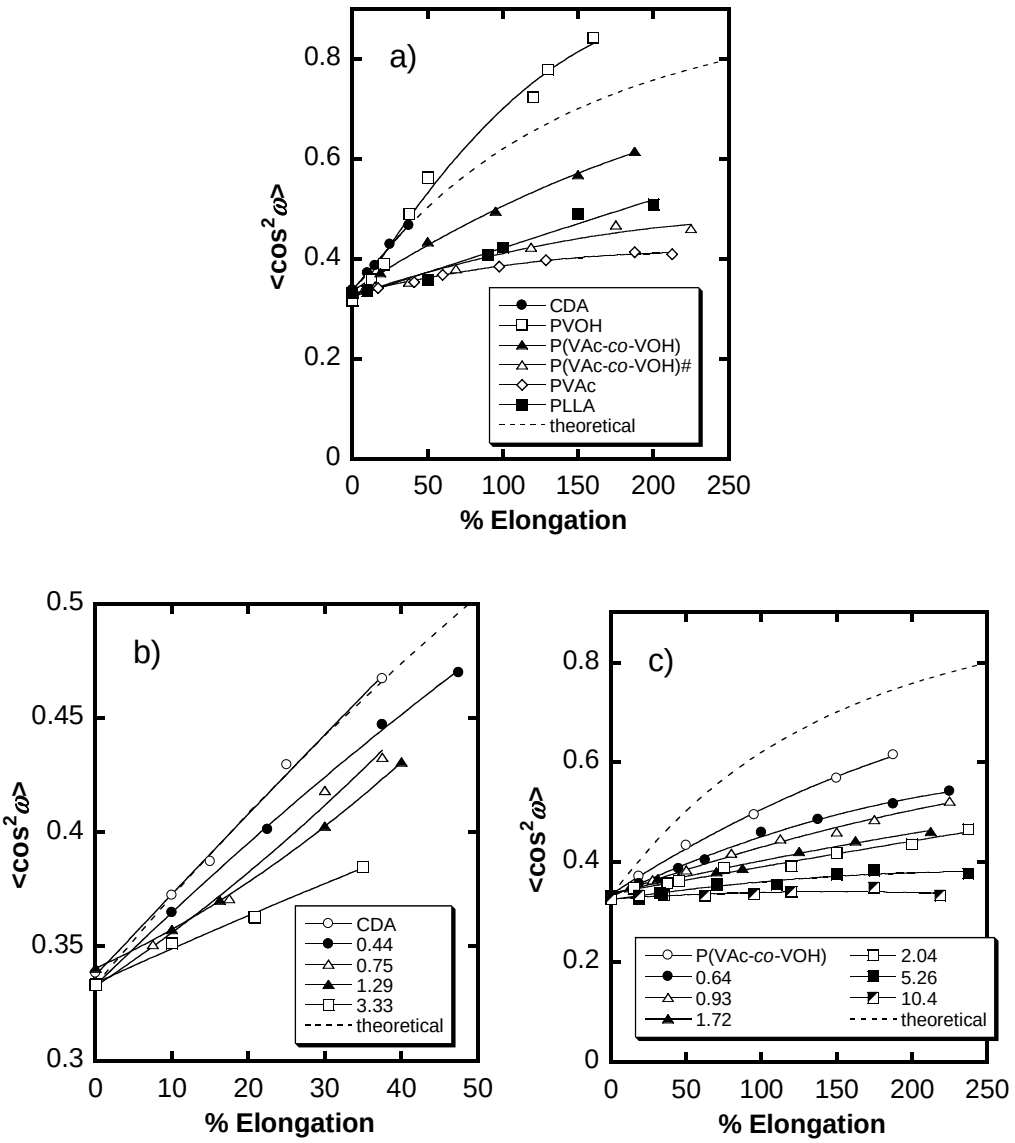
a)
<cos²ω>
% Elongation
CDA
PVOH
P(VAc-co-VOH)
P(VAc-co-VOH)#
PVAc
PLLA
theoretical
b)
<cos²ω>
% Elongation
CDA
0.44
0.75
1.29
3.33
theoretical
c)
<cos²ω>
% Elongation
P(VAc-co-VOH)
0.64
0.93
1.72
2.04
5.26
10.4
theoretical

Figure 4

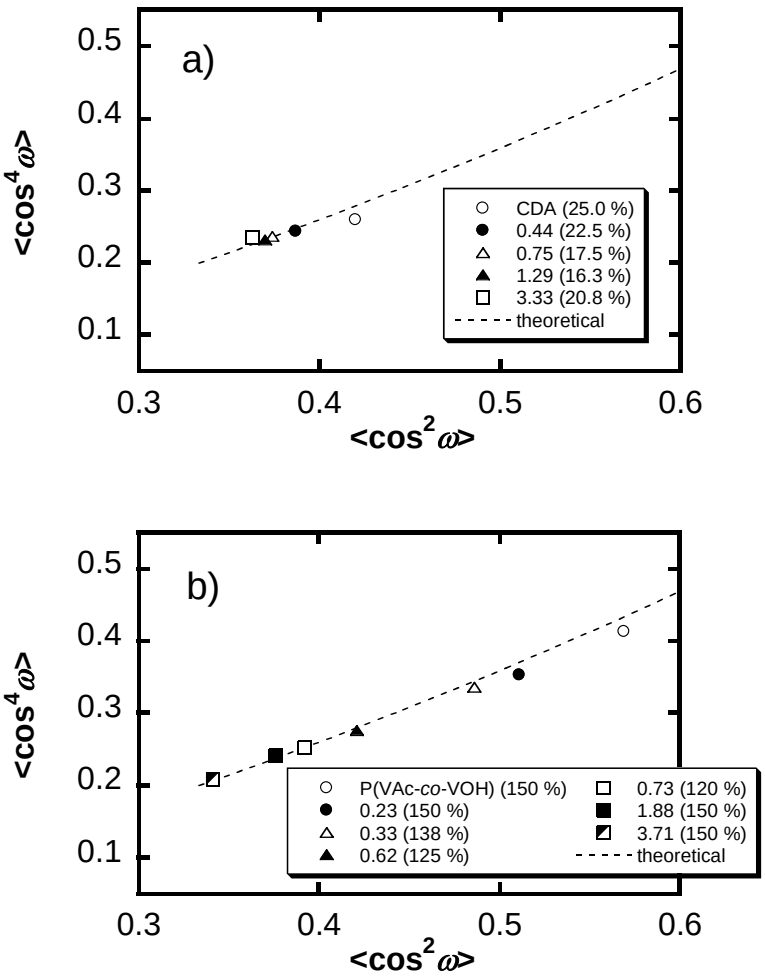
a)
0.5
0.4
0.3
0.2
0.1
0.3
0.4
0.5
0.6
<cos⁴ω>
<cos²ω>
CDA (25.0 %)
0.44 (22.5 %)
0.75 (17.5 %)
1.29 (16.3 %)
3.33 (20.8 %)
theoretical
b)
P(VAc-co-VOH) (150 %)
0.23 (150 %)
0.33 (138 %)
0.62 (125 %)
0.73 (120 %)
1.88 (150 %)
3.71 (150 %)
theoretical

Figure 5

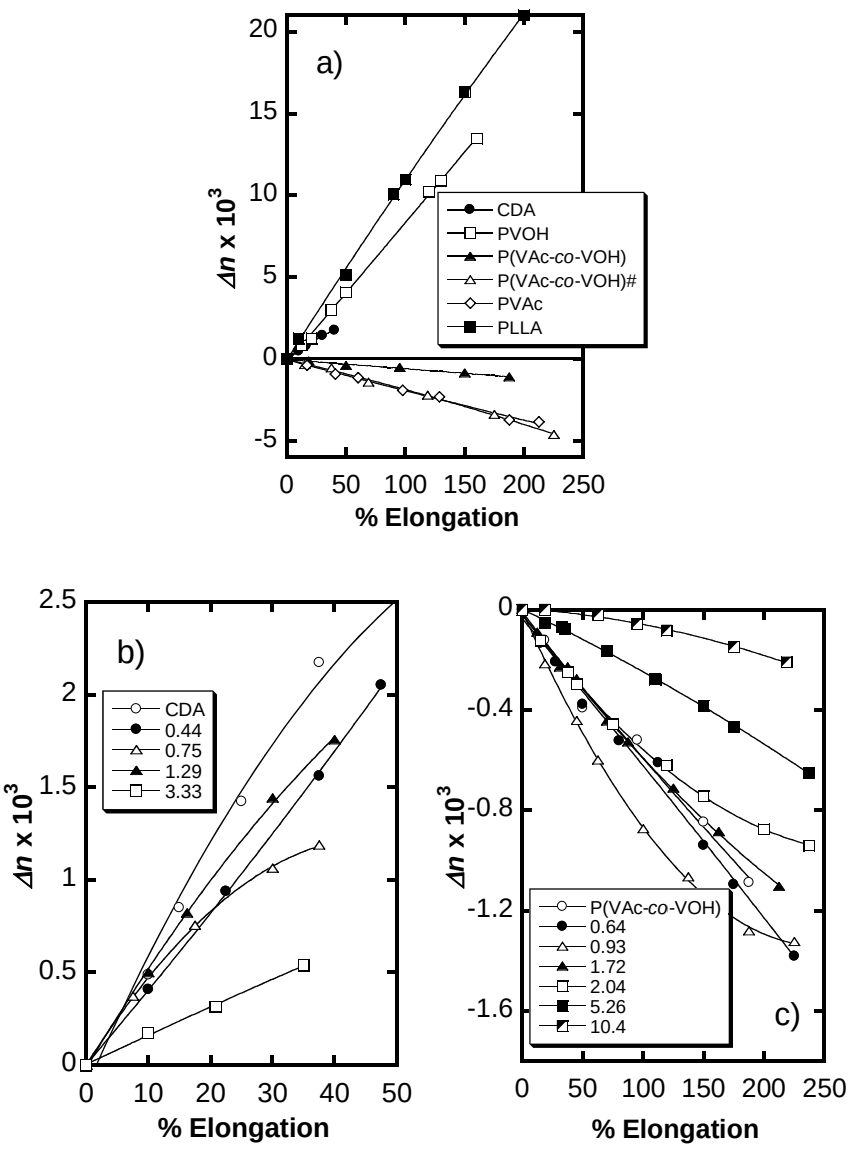
a)
Δn x 10^3
% Elongation
CDA
PVOH
P(VAc-co-VOH)
P(VAc-co-VOH)#
PVAc
PLLA
b)
CDA
0.44
0.75
1.29
3.33
c)
P(VAc-co-VOH)
0.64
0.93
1.72
2.04
5.26
10.4

Figure 6

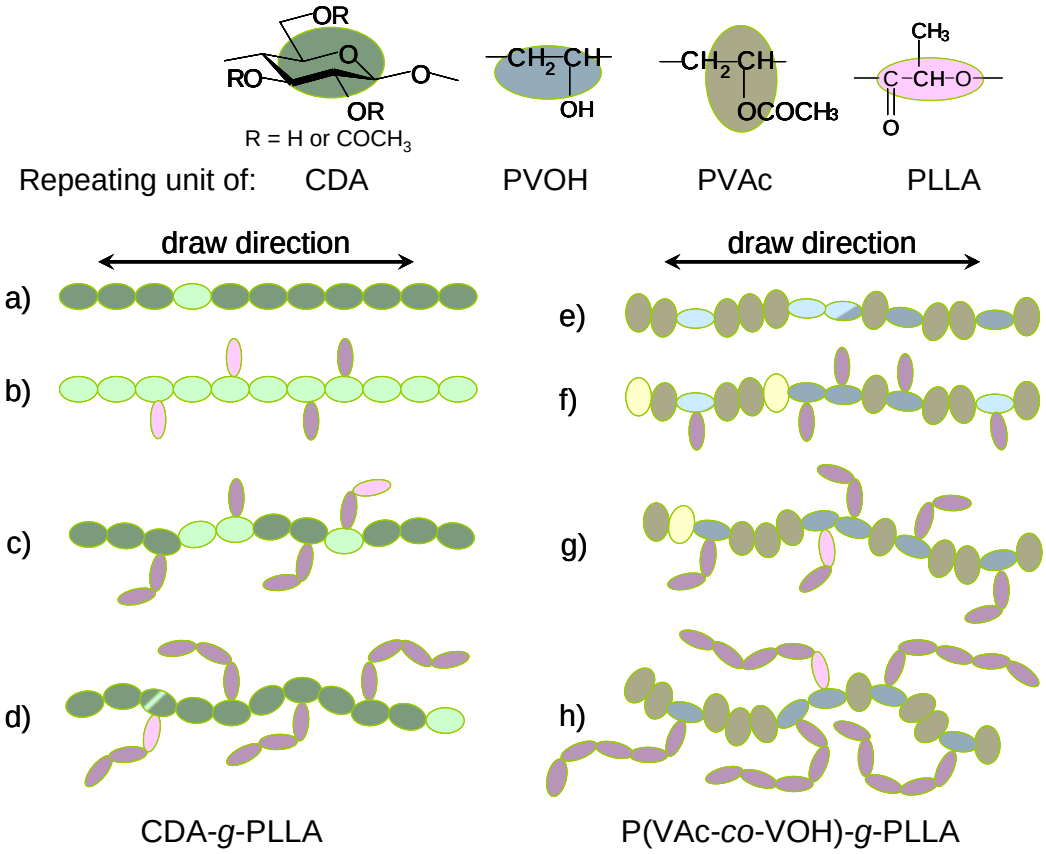
OR
O
RO
O
OR
R = H or COCH3
CH2 CH
OH
CH2 CH
OCOCH3
CH3
C CH O
O
Repeating unit of:
CDA
PVOH
PVAc
PLLA
draw direction
draw direction
a)
b)
c)
d)
e)
f)
g)
h)
CDA-g-PLLA
P(VAc-co-VOH)-g-PLLA

Figure 7